

Measurement of Extinction Coefficients of Laser-Produced Aluminum Plumes

T. E. Mills,* P. J. Bishop,† and A. Minardi‡
University of Central Florida, Orlando, Florida 32816

Radial spectral intensities ($0.632 \mu\text{m}$) were measured using a He:Ne probe laser scanning an aluminum plume formed by Nd:glass laser irradiation of a target surface. Furthermore, techniques were developed to measure the radial distributions of the extinction coefficients in an axisymmetric, laser-produced aluminum plume. The techniques developed allow for measurements of these distributions as functions of time, wavelength, and elevation above the aluminum target. The extinction coefficients determine the ability of the plasma to attenuate incident laser radiation. The extinction coefficient distribution was determined by scanning a He:Ne probe laser through the plume and converting line-of-sight measurements to a radial distribution. Results indicate that the aluminum plume is optically thin in the first $80 \mu\text{s}$ after formation and that the radial extinction coefficient profile has a Gaussian distribution.

Nomenclature

A	= amplitude of Gaussian distribution, dimensionless
I_{emission}	= spectral directional intensity emitted by the plume, $\text{W}/\text{cm}^2 \text{ sr } \mu\text{m}$
$I_{\text{extinction}}$	= spectral directional intensity extinguished by the plume, $\text{W}/\text{cm}^2 \text{ sr } \mu\text{m}$
I_{net}	= net intensity, active-passive, $\text{W}/\text{cm}^2 \text{ sr } \mu\text{m}$
$I_{\text{scattering augmentation}}$	= change in spectral directional intensity by scattering augmentation, $\text{W}/\text{cm}^2 \text{ sr } \mu\text{m}$
I_{total}	= spectral directional intensity at the end of the optical path, $\text{W}/\text{cm}^2 \text{ sr } \mu\text{m}$
i'_{λ}	= spectral directional intensity, $\text{W}/\text{cm}^2 \text{ sr } \mu\text{m}$
$i'_{\lambda}(0)$	= spectral directional intensity entering the plume, $\text{W}/\text{cm}^2 \text{ sr } \mu\text{m}$
$i'_{\lambda,\text{active}}$	= spectral directional intensity measured with the He:Ne probe laser on, $\text{W}/\text{cm}^2 \text{ sr } \mu\text{m}$
$i'_{\lambda,\text{passive}}$	= spectral directional intensity measured with the He:Ne probe laser off, $\text{W}/\text{cm}^2 \text{ sr } \mu\text{m}$
K_{λ}	= extinction coefficient, cm^{-1}
N	= total number of rings for a particular y position
R	= plume radius, mm
r	= radial position, mm
S	= optical path, mm
y	= direction of scans with the probe laser, mm
κ	= optical thickness along the optical path

κ_{λ}	= plasma optical thickness, dimensionless
ω_0	= Gaussian waist, mm

Introduction

THE purpose of this study was to temporally measure the extinction coefficient of a two-dimensional, axisymmetrical cylindrical plume at one wavelength. Knowledge of the radiative properties will aid in the understanding of the radiative heat transfer mechanisms within a laser-produced plume. One theory to explain the physical phenomena of thermal coupling is that very large radiative heat fluxes occur from the plume to the target surface, enhancing the energy that reaches the target. The effective increase in absorptivity of the surface is termed thermal coupling.

As the laser strikes a surface, the material is heated until it is first melted, then vaporized. The vapor absorbs more energy and may form a high-temperature plasma near the surface. The plume can emit, absorb, and scatter incident laser energy. Goncharov and Karaban¹ observed the plume to be cylindrically shaped. Elder et al.² developed a method to measure the absorption and emission coefficients and temperature in a cylindrically symmetric nitrogen plasma column generated by an electric arc. Patel and Brewster³ measured transmittance of a laser-produced plume using a He:Ne probe laser across the plume diameter at a single elevation. Malyshev et al.⁴ used the scattering of a probe laser to determine the electron temperature and number density of a laser-produced air plasma. Goncharov and Karaban¹ used a ruby probe laser to study the absorption and scattering of a laser-produced plasma at different elevations above a target at a particular time using a Nd laser. Two-dimensional temporal measurements of extinction coefficients for a laser-produced plume have not been reported in the literature. Based upon modeling studies of Minardi and Bishop,^{5,6} it is expected that the radiative properties of the plume would vary in a similar fashion with the radial distribution of the incident laser beam.

Mills et al.⁷ examined the role of the plume in thermal coupling by determining the minimum intensity required to vaporize a metal target and compared this to the thermal coupling threshold intensity. A strong correlation was observed between these two intensities and it was concluded that measurement of the radiative properties would explain the role of the plume in laser machining.

This work provides data required to analyze conditions under which the plume formed during laser exposure enhances en-

Presented as Paper 93-3228 at the AIAA 24th Plasmadynamics & Lasers Conference, Orlando, FL, July 6–9, 1993; received Aug. 6, 1993; revision received Nov. 15, 1993; accepted for publication Nov. 16, 1993. Copyright © 1993 by the American Institute of Aeronautics and Astronautics, Inc. All rights reserved.

*Graduate Assistant, Department of Mechanical Engineering, P.O. Box 162450.

†CAE/Link Professor, Department of Mechanical Engineering, P.O. Box 162450.

‡Assistant Professor, Department of Mechanical Engineering, P.O. Box 162450.

ergy delivery to the surface. The physical mechanisms for this enhancement are not fully understood. One of the obstacles to understanding the role of the plume is that the radiative properties, the extinction and absorption coefficients, the scattering coefficient, the temperature distribution, and the scattering phase function of the plume are generally unknown.

The radiative property distributions may provide insight into laser-plume-material interaction processes involved in laser machining of metals. An added benefit of this research is that the input into computer models of thermal coupling of laser energy to metal surfaces will more accurately reflect these properties. The measurement of the extinction coefficient distribution is the first step in an effort currently under way to measure all of the radiative properties in a laser-produced plume.

Formulation of Experimental Technique

The extinction coefficient was determined using a Nd:Glass laser as the incident laser to an aluminum alloy 1100 (99.9% pure) surface. In order to determine the extinction of the plume, a He:Ne probe laser at a wavelength of $0.632 \mu\text{m}$ and known intensity was sent through the plume. The probe laser was passed through the plume at one elevation and various radial positions to obtain a distribution. The attenuation of the probe laser was measured with a high-speed photodetector encased in a light tight case as shown in Fig. 1.

The method for determining extinction coefficients uses the equation of radiative transfer⁸ which can be written as

$$I_{\text{total}} = I_{\text{extinction}} + I_{\text{emission}} + I_{\text{scattering augmentation}} \quad (1)$$

The total intensity exiting a plume along a particular optical path is the sum of external radiation attenuated by the plume according to Bouguer's law, the intensity emitted by the plume into the optical path, and the intensity of radiation scattered into the optical path from other directions.

Equation (1) is applied to two physical situations. The first case, the "passive case," occurs when the probe (He:Ne) laser is not used. The target is irradiated using the incident Nd:Glass laser, and a plume forms. The photodetector will detect the plume emission, but no probe energy passes through the plume to be extinguished. In the second case, the "active case," the probe laser enters the optical path at $\kappa = 0$ as shown in Fig. 2. The geometry shown in the top view of Fig. 2 bears some discussion in that two coordinate systems are used. The radial extinction coefficient profile is obtained at one elevation and the He:Ne laser is scanned across the plume in the y direction. A ring method is used to unfold extinction measurements at different y positions to the radial distribution of the extinction coefficients. The photodetector in the active case records en-

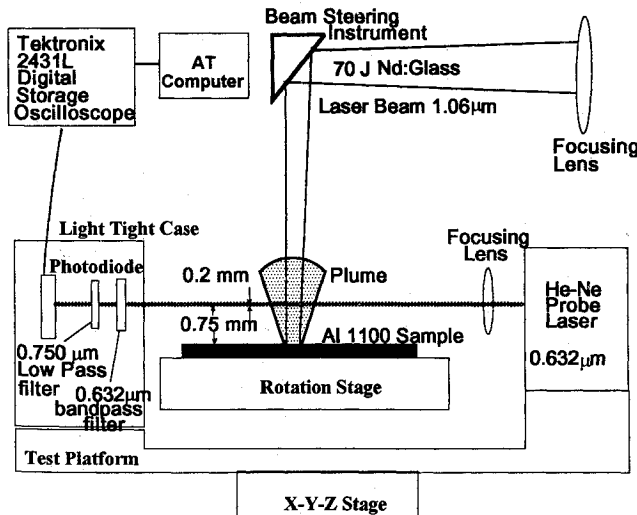


Fig. 1 Experimental setup for measuring extinction coefficients.

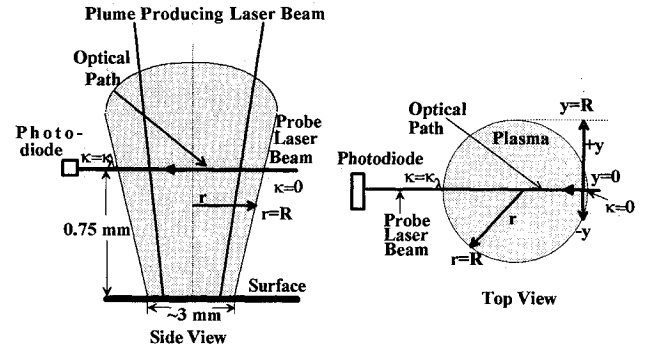


Fig. 2 Extinction pathways for probe (He:Ne) laser. κ is along the optical path of the He:Ne probe laser beam. y is normal to the He:Ne probe laser beam.

ergy received from the plume by emission, scattering augmentation, and the energy from the probe laser that has passed through the plume. The optical pathway for the extinction is from $\kappa = 0$ to $\kappa = \kappa_{\lambda}$. A bandpass filter is used to filter all wavelengths except the $0.632 \mu\text{m}$ produced by the He:Ne laser, and a $0.750\text{-}\mu\text{m}$ low pass filter is used to provide additional blocking of the Nd:Glass laser. The effect of the filters is that radiation of wavelength $0.632 \mu\text{m}$ is the only radiation received by the photodiodes. The equations for the two cases are given as

Case I

$$I = I_{\text{emission}} + I_{\text{scattering augmentation}} \quad (2)$$

Case II

$$I = I_{\text{extinction}} + I_{\text{emission}} + I_{\text{scattering augmentation}} \quad (3)$$

Subtracting Eq. (2) from Eq. (3) gives

$$I_{\text{net}} = I_{\text{extinction}} + I_{\text{emission II}} + I_{\text{scattering augmentation II}} - I_{\text{emission I}} - I_{\text{scattering augmentation I}} \quad (4)$$

Equation (4) can be simplified by realizing that the He:Ne probe laser energy (μJ) is small and does not contribute to heating the plume. This means that plume emission in the two cases will be the same. Also, since the probe laser energy is collimated and the angle of acceptance of the photodiode in the light tight case is less than 0.0008 sr , scattering augmentation could only be important if the probe laser energy were scattered out of the optical path and then rescattered after some multiple scatters directly into the optical path. Approximately $0.05\% \approx (4\pi)^{-3}$ of the incident intensity would be scattered back into the optical path considering three isotropic scatters with no attenuation of energy between points of scatter. Also, the plume is expected to be optically thin so that the intensity of light that is scattered by the plume is small compared to the intensity of light transmitted through the plume. Therefore, if the emission and scattering augmentation terms are approximately the same for both cases I and II, then Eq. (4) reduces to

$$I_{\text{net}} = I_{\text{extinction}} = i'_{\lambda, \text{active}} - i'_{\lambda, \text{passive}} = i'_{\lambda}(0) \exp(-\kappa_{\lambda}) \quad (5)$$

A more convenient form that uses relative values of intensities can be obtained by dividing both sides of Eq. (5) by $i'_{\lambda}(0)$

$$\frac{i'_{\lambda, \text{active}} - i'_{\lambda, \text{passive}}}{i'_{\lambda}(0)} = \exp(-\kappa_{\lambda}) \quad (6)$$

The initial intensity $i'_{\lambda}(0)$ is obtained by measuring the He:Ne intensity just prior to entering the plume. The use of relative

intensities negates the need for conversion of raw data from the photodiodes. Another result of subtracting the passive measurements from the active measurements is that the angle of acceptance of the photodiodes becomes unimportant. Equation (5) shows that the difference of active and passive measurements is the $I_{\text{extinction}}$ term, which is merely the extinction of the He:Ne probe laser. This term contains information only along the collimated optical path of the He:Ne probe laser. The extinction of the He:Ne probe laser is measured at different y positions (as shown in Fig. 2) at an elevation of 0.75 mm above the surface. Scans are obtained by moving the test platform shown in Fig. 1 across the plume so that the radial distribution of extinction coefficients is obtained. A separate laser shot was used for each active and passive measurement at each position. The photodiode signal was stored by the digital oscilloscope, and subsequently transferred to the computer. The oscilloscope was set so that there were 2 μs between each digitized measurement of intensity. Two types of measurements, the active and passive, were taken at each y position (as shown in Fig. 2). After seven active and three passive measurements were obtained, the test platform was moved 0.2 mm in the y direction as shown in Fig. 2. Therefore, 10 separate laser shots were required to obtain the data for each position. This was continued until the temporal profiles of the active and passive measurements were obtained for all positions from $y = 0$ to $y = R$. The diameter of the plume changed with height, and was not known a priori. Therefore, measurements were taken from some-

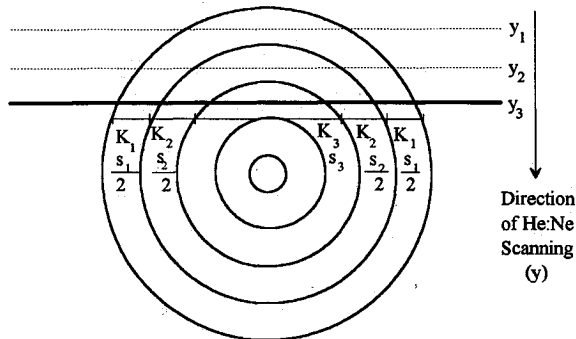


Fig. 3 Path lengths for the ring method.⁹

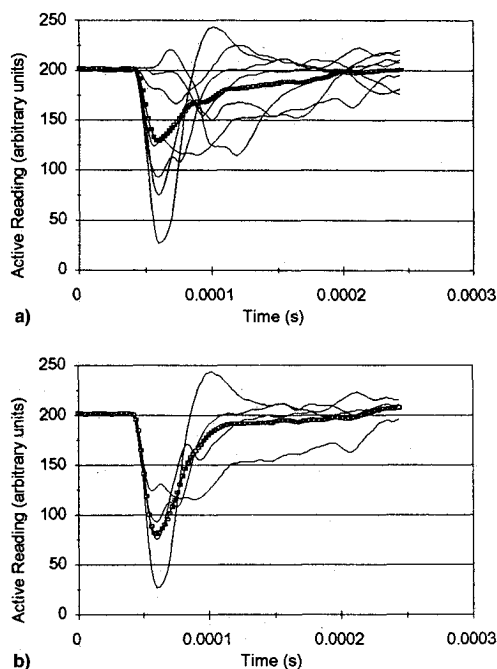


Fig. 4 Active measurement vs time at $y = 0$: a) all data series and b) deviant series removed.

where beyond the center of the plume ($-y$ in Fig. 2) to beyond ($+y > R$ in Fig. 2) the outer edges until no signal was recorded from the plume. The edges were then determined to be at these locations, and due to symmetry, half the diameter located the plume center. Each shot of the Nd:Glass made a hole about 3 mm in diam and about 1 mm deep. The sample was placed on a rotational stage and shots were made in a radial pattern so that a clean surface was exposed to each Nd:Glass laser shot. For consistency, the surfaces were prepared the same by being wet-sanded with 400-grit sandpaper and washed with deionized water, followed by acetone.

To obtain the extinction coefficients, a ring method developed by Cassatta⁹ was employed. This method treats the plume as axisymmetric consisting of a series of constant property rings as shown in Fig. 3. The extinction coefficient is calculated for the outer ring first, and this is used to determine coefficients at each successive interior ring. At each radial location the measurement is composed of the previous rings and the current one. The variation of optical path length through each ring was determined by calculating the path length of each ring at each radial location. Taking the log of both sides of Eq. (6) and substituting for the extinction coefficient in terms of the path length S yields

$$\ln \left(\frac{i'_{\lambda, \text{active}}(0)}{i'_{\lambda, \text{active}}(\kappa_{\lambda}) - i'_{\lambda, \text{passive}}(\kappa_{\lambda})} \right) = \int_0^S K_{\lambda}(s^*) ds^* \\ \approx \sum_{i=1}^N K_{\lambda,i}(S_i) S_i \quad (7)$$

The initial intensity entering the plume was measured in the active case. The change of intensity through the plume was the difference in intensity between the active and passive cases. $K_{\lambda,i}$ is the extinction coefficient of each individual ring, S_i is the length of the optical path of each individual ring, and N is the total number of rings from the plume edge to the y position of interest. The assumption in using the ring method is that the plume is optically thin and does not cause refraction of the light from the pathway. McKay et al.¹⁰ found the difference of the index of refraction of a laser-produced aluminum plume compared to air to be on the order of 10^{-3} . Cheng and Casperson¹¹ found that the maximum deflection of a He:Ne beam by a laser-produced aluminum plasma is less than 0.5 mrad.

Experimental Apparatus

The experimental setup is shown in Fig. 1. A 70-J Nd:Glass laser was focused at the aluminum surface and fired. The Nd:Glass laser was focused to obtain spectral, total intensity levels of $5 \times 10^5 \text{ W/cm}^2 \mu\text{m}$. The pulse length of the laser was about 2 ms, composed of microsecond spikes superimposed in a train throughout the pulse. The pulse spikes vary by less than 5% in magnitude and have a phase shift (in μs) from shot to shot, although the Nd:Glass laser beam was found to be repeatable when averaged. This repeatability is important due to the number of shots required to complete a data scan. The probe laser was passed through the plume and captured by a photodiode. The photodiode signal was received at an oscilloscope where the speed was set at 2 μs per digitized point.

Three passive and seven active measurements were taken at each position and separately averaged to reduce the variability in the data. The repeatability of the passive measurements was good. However, there was some variance in the active data. For this reason, more active measurements were obtained. To reduce the total number of measurements needed for the active case, data sets that did not follow the trends of the other data sets were eliminated. The elimination criteria was based upon two factors: 1) repeatability of the data at a particular y position, and 2) repeatability with data at adjacent y positions. These criteria were applied in the following man-

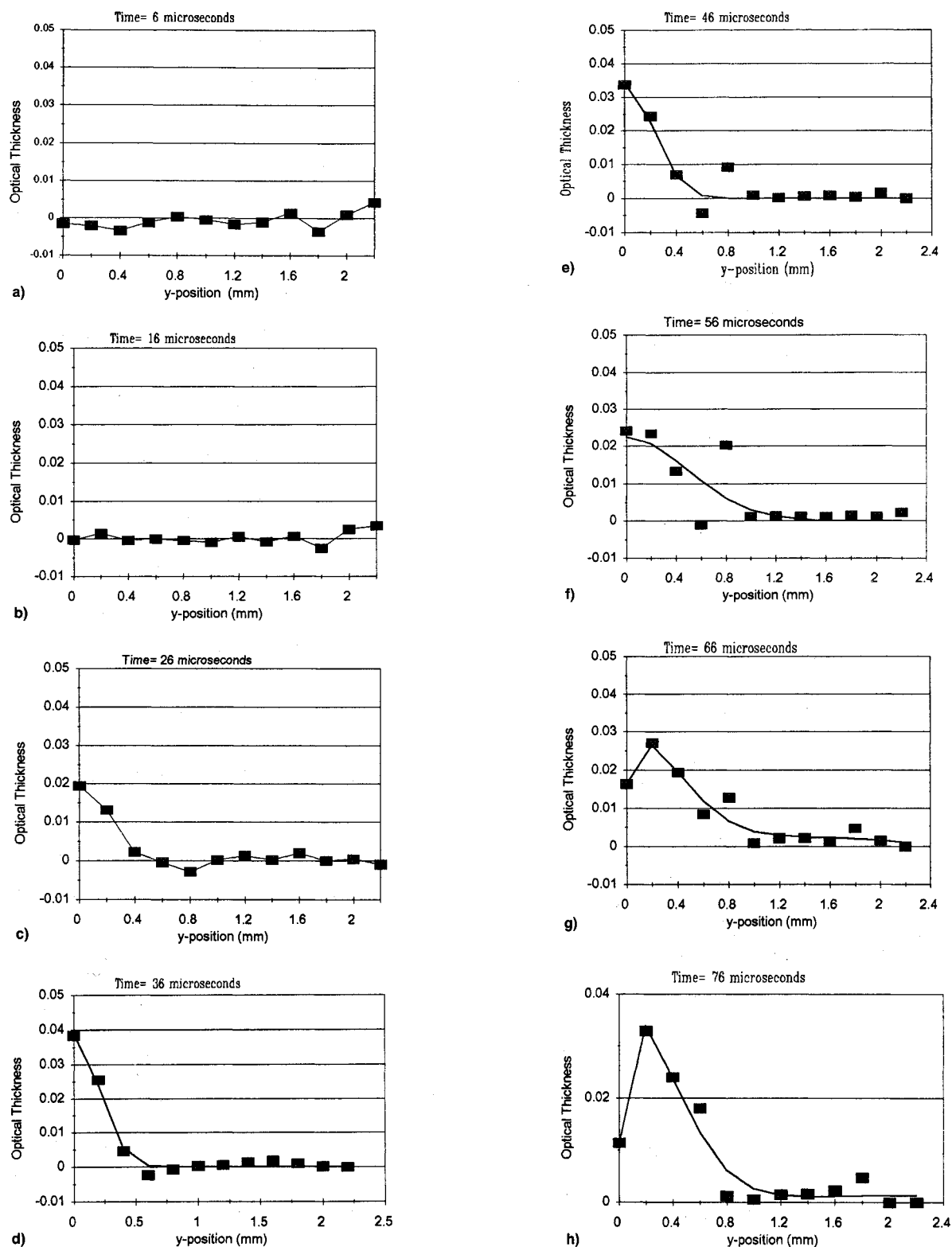


Fig. 5 Optical thicknesses at various times: a) 0–10 μ s, b) 10–20 μ s, c) 20–30 μ s, d) 30–40 μ s, e) 40–50 μ s, f) 50–60 μ s, g) 60–70 μ s, and h) 70–80 μ s.

ner. First, all of the data sets at a particular y position were graphed together along with the average of all data. The data set that was the most deviant from the average was removed and the average was recalculated.

This was continued until the average set of data was composed of a number of similar data sets. If there was some question as to which data set was the most deviant, the data from an adjacent y position was used to give additional information by comparing intensity information at the current

y position to the intensity information at the previous y position. In most cases, two sets of data were eliminated, leaving five.

It was observed during the course of the incident laser pulse, that molten material was expelled from the hole that was drilled. This has been observed by Bass et al.¹² and Goncharov and Karaban.¹ Cover glasses were needed all around the test area to protect the optics from damage. In an earlier study, Mills¹³ concluded that liquid droplet formation at later times

during the laser pulse cause additional extinction of the probe laser beam, rendering the techniques developed here unsatisfactory.

Results and Discussion

Figure 4 shows the raw active data obtained through the center ($y = 0$ in Fig. 2) of the plume. Figure 4a shows all series with the average highlighted by markers, and Fig. 4b shows the data series remaining after deviant series were re-

moved with the average highlighted by markers. The laser fires at approximately $10 \mu\text{s}$.

Figure 5 shows the optical thickness (unitless) at the different y locations obtained from Eq. (7). The y position is in millimeters, and a y position of 0 mm corresponds to the center of the plume. Increasing values of y position show movement away from the center of the plume. All graphs shown are time averaged. The average of five oscilloscope points, two above the center and two below, are used for each graph. Therefore, with a time between each oscilloscope point of $2 \mu\text{s}$, each graph covers a time interval of $10 \mu\text{s}$. Figure 5a represents $6 \mu\text{s}$ after the Nd:Glass laser is fired, whereas each succeeding graph is $10 \mu\text{s}$ later. Later times are not shown. The reason for this will be forthcoming.

Figures 5a and 5b show no extinction. This implies that at these times, the plume has not formed at the elevation at which the data was taken, 0.75 mm above the surface. This is in agreement with Mills et al.⁷ (1991) who calculated that the plume forms at the surface at least $10 \mu\text{s}$ after the laser has fired for the intensity level. The plume would require additional time to travel to an elevation of 0.75 mm. Figures 5c and 5d show extinction at the center of the plume (y position of 0 mm) that falls off quickly towards the edges. Figures 5e and 5f also show extinction at the center of the plume that falls off towards the edges with slight increases at y positions of 0.6 and 0.8 mm. These increases also appear at the same position in Fig. 5g. To obtain extinction coefficients, the best fit line was drawn through the optical thickness data shown in Figs. 5c–5h. The source of these increases in optical thickness is believed to be liquid droplets which are observed at later times. In Figs. 5c–5h, the markers are the original data and the lines without markers are the curve-fitted data. In each case (with a slight exception in Fig. 5d), the best fit was a Gaussian profile $\{A \exp[-(r^2/\omega_0^2)]\}$. This has some implications that will be discussed later. It should be noted that in Fig. 5d, the center point in the fit was kept the same as the raw data, and all other points were given a Gaussian fit.

The optical thickness of the plume never exceeded 0.05 for the times shown at this elevation. This means that the plume is optically thin, which agrees with the results of Knudtson et al.¹⁴ Patel and Brewster³ observed a transmittance of 0.95 at about $50 \mu\text{s}$ for a laser-produced plume obtained at a spectral, total laser intensity of 10^6 W/cm^2 . This corresponds to an optical thickness of 0.05.

Information on the variation of plume size with time can also be inferred from Fig. 5. The edge of the plume can be identified as the first position where the optical thickness is zero. By applying this criteria, one sees that the plume radius is 0.4 mm between 20–30 μs after the laser has fired, 0.6 mm between 30–40 μs , 0.6 mm between 40–50 μs , 0.6 mm between 50–60 μs , 1.0 mm between 60–70 μs , and 0.8 mm between 70–80 μs .

This optical thickness data was used to calculate the radial distribution of the extinction coefficients by using Eq. (7). These distributions are shown in Fig. 6. In Fig. 6a, raw (i.e., not curve-fitted) data was used. The variation in this graph represents experimental error. It should not be inferred that the extinction coefficient is negative. A negative extinction coefficient in this graph are due to experimental error. In the rest of the graphs, the curve-fitted optical thicknesses from Fig. 5 were used. The extinction coefficients for the times prior to those shown in Fig. 6 are essentially zero as is shown by Figs. 5a and 5b, which have optical thicknesses of essentially zero. Between 20–50 μs , the profile of the extinction coefficients closely follows a Gaussian distribution, $A \exp[-(r^2/\omega_0^2)]$. This result has significance because the Nd:Glass laser was operating approximately in a TEM₀₀ mode, a Gaussian distribution of laser beam intensity. This may imply that the distribution of extinction coefficients follows the mode of the laser beam at the early times. Minardi and Bishop⁵ suggested from modeling studies that the properties and temperature

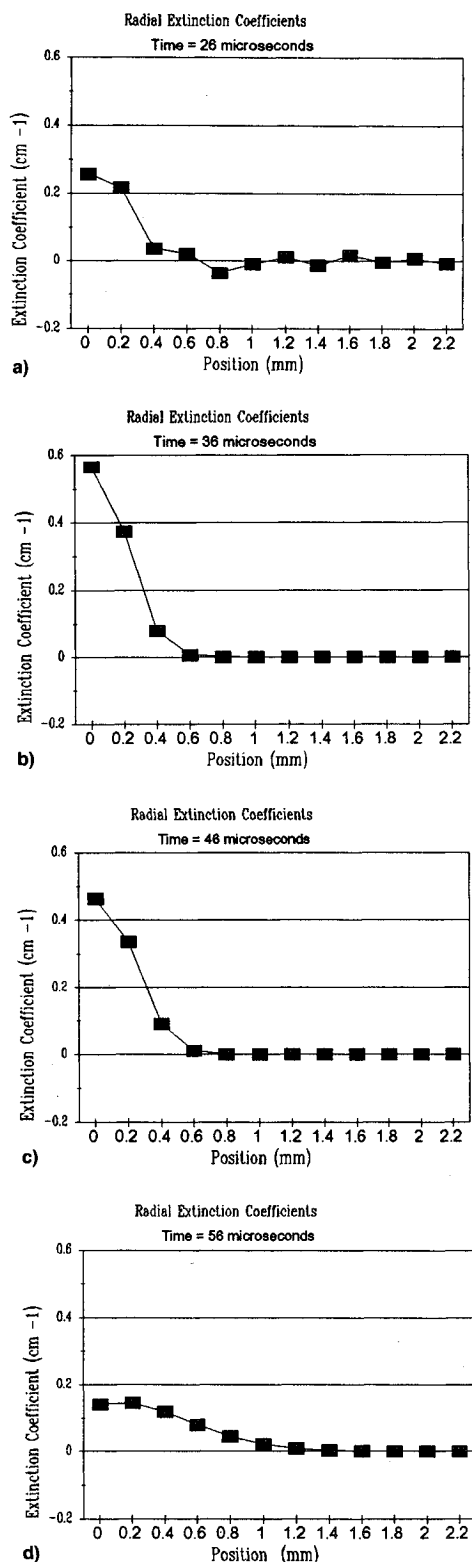


Fig. 6 Radial profile of the extinction coefficient at various times: a) 20–30 μs , b) 30–40 μs , c) 40–50 μs , and d) 50–60 μs .

distribution would follow the laser beam profile. The amplitude of the extinction coefficient begins growing between 20–30 μs , peaks between 30–40 μs , and decays between 40–60 μs . This is due to the plume moving up the Nd:Glass laser beam. This movement was observed by Stegman et al.¹⁵ and McKay et al.¹⁰ As the plume travels up the laser beam and separates from the surface, the extinction near the surface decreases.

Another interesting feature can be observed between 50–60 μs . The extinction coefficient at the center of the plume is actually lower than the extinction coefficient at 0.2 mm from the center. This off-axis peak in the extinction coefficient is not unexpected. Mills¹² found a similar off-axis peak in the absorption coefficient distribution of an aluminum plume produced with a laser beam intensity of 10^6 W/cm^2 , 3 mm above the surface 250 μs after the laser was fired. The extinction coefficient is the sum of the absorption and scattering coefficients, and therefore, since the absorption coefficient shows off-axis peaks, the extinction coefficient may also show an off-axis peak. This behavior may be understood by examining the radial temperature distribution. Cassatta⁹ showed that the radial temperature distribution follows the absorption coefficient distribution. The off-axis peak temperature is caused by the symmetric nature of the Gaussian beam, which in the radial direction results in zero radiative fluxes at the center and edges. Therefore, the maximum flux and temperature must occur somewhere between these locations.

At later times the extinction coefficient at the plume center ($y = 0$) becomes strongly negative. We believe the reason the extinction coefficient goes negative is that liquid droplets are present within the plume. This causes excess extinction of the probe laser beam. Lumpp and Allen¹⁶ reported a plume wave from an aluminum surface irradiated by a laser followed by a material wave. The material wave was in the form of liquid droplets. Droplets are opaque to radiation and cause extinction of the He:Ne probe laser. The ring method by which the optical thicknesses are converted to extinction coefficients starts at the edge of the plume and then works towards the center. This means that when a droplet has interfered with the probe laser at a position near the edge, the value of the extinction coefficient will be underestimated towards the center. This underestimation can reach the point where negative extinction coefficients are obtained. It is clear that the measurement technique breaks down at later times when liquid droplets are present.

Summary

Extinction coefficients of laser-produced aluminum plumes were measured as a function of radial position and time at one elevation. It was found that the extinction coefficients decreased with radial distance from the laser beam center. The plume, within the first 80 μs , was optically thin with maximum extinction coefficients of 0.6 cm^{-1} at the laser beam center as observed in Fig. 6b. This corresponds to an optical thickness of about 0.04.

The extinction coefficients were measured at the wavelength of the He:Ne probe laser ($0.632 \mu\text{m}$). The choice of wavelength was made due to the cost efficiency and ease of operation provided by He:Ne lasers. This experimental work, although limited to a single wavelength, is the first to measure radial profiles of extinction coefficients and provides a first estimate of the extinction coefficient profiles for the entire plume. These measurements are necessary to understand laser-plume-material interactions. Knowing the radiative properties of the plume allows calculation of the radiative fluxes to the surface during laser machining processes. It would be useful to obtain radiative properties at other wavelengths, including

that of the plume producing laser. The techniques developed here to determine extinction coefficients cannot be used for longer times when liquid droplets are present in high concentrations.

Acknowledgments

The authors would like to thank the National Science Foundation for a Graduate Fellowship, the Florida Space Grant Consortium, and UCF-CREOL (the Center for Research in Electro-Optics and Lasers) for their support of this study.

References

- ¹Goncharov, V. K., and Karaban, V. I., "Variation of the Indices of Absorption and Scattering Along a Laser Erosion Torch," *Zhurnal Prikladnoi Spektroskopii*, Vol. 45, No. 1, 1986, pp. 22–25.
- ²Elder, P., Jerrick, T., and Birkeland, J. W., "Determination of the Radial Profile of Absorption and Emission Coefficients and Temperature in Cylindrically Symmetric Sources with Self Absorption," *Applied Optics*, Vol. 4, No. 5, 1965, pp. 589–592.
- ³Patel, R. S., and Brewster, M. Q., "Effect of Oxidation and Plume Formation on Low Power Nd:Yag Laser Metal Interaction," *Journal of Heat Transfer*, Vol. 112, Feb. 1990, pp. 170–177.
- ⁴Malyshev, G. M., Razdobarin, G. T., and Semenov, V. V., "Determination of Parameters of Laser-Induced Plasma in Air by a Scattering Method," *Soviet Physics-Technical Physics*, Vol. 17, No. 7, 1973, pp. 1137–1139.
- ⁵Minardi, A., and Bishop, P. J., "Temperature Distribution Within a Metal Subjected to Irradiation by a Laser of Spatially Varying Intensity," *Heat Transfer in Manufacturing and Materials Processing*, Vol. 113, American Society of Mechanical Engineers Heat Transfer Div., New York, July 1989, pp. 39–44.
- ⁶Minardi, A., and Bishop, P. J., "Computer Modeling of Thermal Coupling Resulting from Laser Irradiation of a Metal Target," *Journal of Materials Processing and Manufacturing*, Vol. 1, No. 3, 1993, pp. 273–294.
- ⁷Mills, T. E., Minardi, A., and Bishop, P. J., "A Comparison of Thermal Coupling Threshold Intensities to Minimum Vaporization Intensities for Metals Subject to Laser Irradiation," *Heat Transfer in Metals and Containerless Processing and Manufacturing*, Vol. 162, American Society of Mechanical Engineers Heat Transfer Div., 1991, pp. 67–73.
- ⁸Siegel, R., and Howell, J. R., *Thermal Radiation Heat Transfer*, Hemisphere, New York, 1981, pp. 454, 455.
- ⁹Cassatta, J. A., "Determination of Radiative Properties in a Radially Symmetric Plasma Column from Remote Spectral Scanning by Spectroscopy and Photodetection," M.S.M.E. Thesis, Univ. of Central Florida, Orlando, FL, 1991.
- ¹⁰McKay, J. A., Bleach, R. D., Nagel, D. J., Schriempf, J. T., Hall, R. B., Pond, C. R., and Manlief, S. K., "Pulsed CO₂ Laser Interaction with Aluminum in Air: Thermal Response and Plasma Characteristics," *Journal of Applied Physics*, Vol. 50, No. 5, 1979, pp. 3231–3240.
- ¹¹Cheng, T. K., and Casperson, L. W., "Plasma Diagnosis by Laser Beam Scanning," *Journal of Applied Physics*, Vol. 46, No. 5, 1975, pp. 1961–1965.
- ¹²Bass, M., Nassar, M. A., and Swimm, R. T., "Impulse Coupling to Aluminum Due to Long Pulse Nd:Glass Laser Irradiation," *Journal of Applied Physics*, Vol. 61, No. 3, 1987, pp. 1137–1144.
- ¹³Mills, T. E., "The Measurement of the Radial Distribution of Extinction, Absorption, and Scattering Coefficients of Aluminum Plasmas Produced by a Nd:Glass Laser," M.S.M.E. Thesis, Univ. of Central Florida, Orlando, FL, 1992.
- ¹⁴Knudtson, J. T., Green, W. B., and Sutton, D. G., "The UV-Visible Spectroscopy of Laser Produced Aluminum Plasmas," *Journal of Applied Physics*, Vol. 10, No. 10, 1987, pp. 4771–4780.
- ¹⁵Stegman, R. L., Schriempf, J. T., and Hettche, L. R., "Experimental Studies of Laser-Supported Absorption Waves with 5-ms Pulses of 10.6- μ Radiation," *Journal of Applied Physics*, Vol. 44, No. 8, 1973, pp. 3675–3681.
- ¹⁶Lumpp, J. K., and Allen, S. D., "Laser Micromachining of AlN," *Proceedings of the International Conference on Beam Processing of Advanced Materials*, TMS/ASM 1992 Fall Meeting, The Metals Society, Warrendale, PA, 1992, pp. 201–210.